Construction Wind Loading for Steel Girders – Resiliency and Reliability

FINAL REPORT

Date: April 11, 2023

By: Elsayed Eshra,
Gordon Warn,
Konstantinos Papakonstantinou

Pennsylvania State University

COMMONWEALTH OF PENNSYLVANIA
DEPARTMENT OF TRANSPORTATION

CONTRACT #4400023298
WORK ORDER # PSU 010

Technical Report Documentation Page

1. Report No. FHWA-PA-2023-003-PSU WO 010	2. Government Accession No.	3. Recipient's Catalog No.	
4. Title and Subtitle Construction Wind Loading for Steel Girders – Resiliency and Reliability		5. Report Date April 11, 2023	
		6. Performing Organization Code	
7. Author(s) Elsayed Eshra**,** Gordon Warn**,** and Konstantinos Papakonstantinou Pennsylvania State University		8. Performing Organization Report No.	
9. Performing Organization Name and Address The Pennsylvania State University College of Engineering Department of Civil and Environmental Engineering 212 Sackett Building University Park, PA 16802-1408		10. Work Unit No. (TRAIS)	
		11. Contract or Grant No. **4400023298-512101 PSU WO 010**	
12. Sponsoring Agency Name and Address The Pennsylvania Department of Transportation Bureau of Planning and Research Commonwealth Keystone Building 400 North Street, 6th Floor Harrisburg, PA 17120-0064		13. Type of Report and Period Covered Research report. 18 April 2022 to 18 April 2023	
		14. Sponsoring Agency Code	
15. Supplementary Notes			

16. Abstract
The main objective of this study is to assess and evaluate PennDOT's current specifications for wind loading on completely erected steel girders with diaphragms installed but prior to the placement of the deck. Current specifications are evaluated with respect to recent changes to AASHTO's wind loading procedures for bridges under construction based on the 3-second wind gust calculations and the relevant state-of-art research. This report first provides a comprehensive literature review on wind loading for bridges under construction, including the relevant PennDOT wind loading procedures and lateral stability bracing guidelines. Subsequently, the PennDOT wind loading procedures are comparatively examined against the corresponding AASHTO procedures. The structural modeling and analysis procedures, utilized to evaluate the relevant PennDOT's lateral stability bracing guidelines, are then developed and verified. A parametric study was implemented to assess these guidelines, considering all relevant parameters involved in wind loading, structural modeling, and analysis. Numerous girder systems with different parameter values were analyzed, with a particular emphasis on comparing the lateral displacement of the girder systems against the permissible values. Additional investigations are subsequently discussed to explore the effect of fully and partially fixed transverse diaphragm connections, as well as variations in the diaphragms' and braces' cross-section size, on the lateral displacement of girder systems. The impact of the uplift wind forces on system demands is also examined. Based on the findings of this study, it is determined that the current PennDOT's wind loading procedure is slightly more conservative than AASHTO's wind loading procedures for bridges under construction for the typical cases of bridges with 4, 5 and 6 main girders and girder spacing to girder depth less than or equal to 3. It is also concluded that lateral stability bracing can be required for bridges with girder span lengths greater than or equal to 150 ft.

17. Key Words Bridges under construction, wind loading, lateral stability bracing, steel girders	18. Distribution Statement No restrictions. This document is available from the National Technical Information Service, Springfield, VA 22161		
19. Security Classif. (of this report) Unclassified	20. Security Classif. (of this page) Unclassified	21. No. of Pages 39	22. Price $93,858.05

Form DOT F 1700.7   **(8-72)**   **Reproduction of completed page authorized**

Disclaimer

The contents of this report reflect the views of the authors who are responsible for the facts and the accuracy of the data presented herein. The contents do not necessarily reflect the official views or policies of the US Department of Transportation, Federal Highway Administration, or the Commonwealth of Pennsylvania at the time of publication. This report does not constitute a standard, specification, or regulation.

Credit

Table of Contents

Chapter 1 Introduction

1.1 Background

The current PennDOT specifications outline wind loading procedures and lateral stability bracing for bridges under construction. Over the years, these specifications have been updated to align with contemporary research findings (PennDOT 2010, 2016, 2019a, 2019b, 2020). The current PennDOT specification entails a unique combination of different wind loading procedures, including the National Highway Institute (NHI) course number 130102 (NHI 2015) and AASHTO Guide Specification for Wind Loads During Construction (AASHTO 2017). Consequently, it is necessary to comprehensively evaluate and assess the relevant PennDOT specification based on recent standards, specifications, and state-of-the-art research (AASHTO 2017, 2020; Consolazio et al. 2013; Wassef and Raggett 2014).

1.2 Problem Statement and Project Objective

The objective of this project is to assess and evaluate PennDOT's current specifications for wind loading on completely erected steel girders with diaphragms installed but prior to the placement of the deck. Current specifications are evaluated with respect to recent changes to AASHTO's wind loading procedures for bridges under construction based on the 3-second wind gust calculations and the relevant state-of-art research.

1.3 Organization

This report consists of five chapters. The remaining chapters cover the following topics:

Chapter 2 provides a comprehensive literature review on the wind loading for bridges under construction, in particular the expressions and values for the wind loading parameters in the relevant standards and specifications. The relevant PennDOT wind loading procedures and lateral stability bracing guidelines are subsequently discussed.

Chapter 3 develops the structural modeling and analysis procedures utilized to evaluate PennDOT's lateral stability bracing for bridges' steel girder systems prior to the placement of the deck. The details of the structural modeling are first provided, by showing the considered structural elements, supports, and connections, in addition to the structural analysis procedures. A case study bridge girder system is analyzed, to provide an example of wind loading and structural modeling and analysis, and importantly to verify the considered structural modeling and analysis procedures. Additional investigations are then discussed to explore the effect of rigid and partially fixed transverse diaphragm connections, as well as variations in the diaphragms' and braces' cross-section size, on the lateral displacement of girder systems. The impact of the uplift wind forces on system demands is also examined.

Chapter 4 implements a parametric study to further assess the PennDOT lateral stability bracing guidelines, considering all relevant parameters involved in wind loading, structural modeling, and analysis. Numerous girder systems with different parameter values are analyzed, with a particular emphasis on comparing the lateral displacement of the girder systems against the permissible values. A comprehensive analysis of the parametric study results is also provided.

Finally**, Chapter 5** summarizes the report and lists the key findings, contributions, and recommendations.

Chapter 2 Literature Review

2.1 Introduction

This study is concerned with the assessment and evaluation of the PennDOT's current specifications for wind loading on completely erected steel superstructures with diaphragms installed but prior to the placement of the deck. The PennDOT Bridge Standard BD-620M (PennDOT 2019a) provides wind loading procedure and lateral stability bracing guidelines for the steel superstructures at the targeted construction stage, which will be referred to as girder systems hereafter. The National Highway Institute (NHI) course number 130102 (NHI 2015) is the reference for the PennDOT wind loading procedure provided in PennDOT BD-620M (PennDOT 2019a). Additionally, the PennDOT Publication 408/2020 for construction specifications (PennDOT 2020) mentions that during erection of a bridge superstructure, the wind loads and distribution of wind loads to the girders shall follow the AASHTO Guide Specifications for Wind Loads During Construction (AASHTO 2017).

In this chapter, the wind loading for bridges under construction is first discussed, in particular the expressions and values for the wind loading parameters in the relevant standards and specifications (AASHTO 2017; ASCE/SEI 2022; NHI 2015). The PennDOT wind loading procedures and lateral bracing guidelines provided in PennDOT BD-620M (PennDOT 2019a) are subsequently discussed. A comparison between the wind pressure computed according to these references is also shown for an illustrative example.

2.2 Wind Loads on Bridges During Construction

2.2.1 General overview

The general mathematical form for computing the wind pressure on bridges during construction, used by many design specifications and discussed subsequently, is as follows:

$$P_z = 2.56 * 10^{-3} V^2 R^2 K_z G C_D \tag{1}$$

where: P_z: is the design wind pressure in psf; V: the basic design wind speed in mph defined as the 3-sec gust wind speed at 33 ft above the ground in open terrain in contemporary design specifications/codes (wind exposure category C in (ASCE/SEI 2022)); R: is a reduction factor to the design wind speed according to the expected construction duration; K_z: is an exposure and elevation factor, accounting for the effect of the elevation of the studied structure or bridge, site topography, and surrounding obstructions on wind speed profile; G: is a gust effect factor, accounting for the effect of the distribution of gust wind pressure over the structure and structural dynamic effects on peak structural response; and C_D: is a drag coefficient, a dimensionless quantity that relates the pressure on an object to its shape and size.
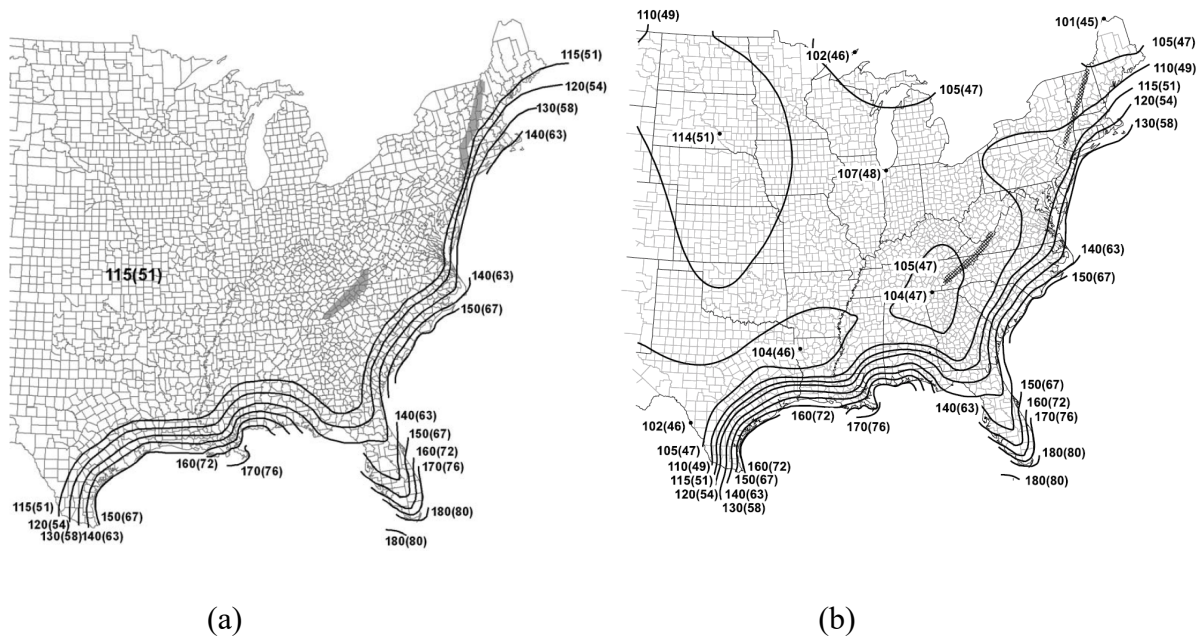
Figure 2.1: Design wind speed map corresponding to an MRI of 700 years (mph): (a) ASCE 7-10 (ASCE/SEI 2010); (b) ASCE 7-22 (ASCE/SEI 2022).

2.2.2   Design wind speed (V)

The 3-sec gust basic wind speed maps provided in ASCE 7-10 (ASCE/SEI 2010) are currently the most widely used to determine the basic design wind speed, V, in the U.S. (AASHTO 2017, 2020). The 3-sec gust basic wind speeds were intended to be used with a load factor (LF) equal to 1.0. (ASCE/SEI 2010) provided four maps corresponding to mean recurrence intervals (MRIs) of 300, 700, 1,700, and 3,000 years, based on the risk category of the structure. A detailed explanation of the ASCE 7-10 design wind speed maps that have been developed can be found in (Vickery et al. 2010). They showed how the basic relationship for wind speeds, in non-hurricane regions of the U.S., with various MRIs developed by Peterka and Shahid (1998), is used to estimate the MRI corresponding to LF of 1.0 for each ASCE 7 risk category.

In 2015, AASHTO (AASHTO 2015) changed their wind loading guidelines considerably from the fastest-mile measure of wind speed to the 3-sec gust wind, mainly based on work by Wassef and Raggett (2014). Up to that time, for the basic design wind speed, V, AASHTO implicitly used a load factor (LF) of 1.4 with an MRI of 100 years (Wassef and Raggett 2014). Inspired by (ASCE/SEI 2010), (AASHTO 2015) changed the wind LF from 1.4 to 1.0, which, together with other modifications, as shown subsequently, was equivalent, for all practical purposes, to the prior wind load levels based on an MRI of 100 years and an LF of 1.4. Based on the expression provided by Simiu and Scanlan (1997) for computing wind speed as a function of MRI, Wassef and Raggett (2014) showed that the design wind speed corresponding to MRI of 100 years with an LF of 1.4 is equivalent to the 3-sec gust design wind speed provided in ASCE 7-10 wind speed map for MRI

of 700 years and an LF of 1.0. Consequently, AASHTO LRFD Bridge Design Specifications (AASHTO 2015) adopted this ASCE 7-10 design wind speed map, shown in Figure 2.1(a).

Similarly, the National Highway Institute (NHI) course number 130102 (NHI 2015), which is the reference for PennDOT wind loading on bridges during construction (PennDOT 2019a), adopted the same ASCE 7-10 design wind speed map. As can be seen in Figure 2.1(a), the design wind speed for Pennsylvania is 115 mph. Recently, ASCE 7-22 (ASCE/SEI 2022) provided an updated version of the chosen design wind speed map, shown in Figure 2.1(b), noting the maximum design wind speed for Pennsylvania remained 115 mph and a finer spatial estimate is now available, that might be useful when a site-specific study is performed.

2.2.3   *Wind speed reduction factor (R)*

A design wind speed with an MRI of 700 years corresponds to approximately a 7% probability of exceedance in 50 years. For bridges under construction, the period between the erection of the girders and the placement of the deck is expected to be short in comparison to the lifespan of the bridge. Given this, the design wind speed decreases with the decrease of the considered time duration for the same probability of exceedance, hence the design wind speed provided in the ASCE 7-10 map, adopted by recent AASHTO specifications (AASHTO 2017, 2020), is to be adjusted for wind loads during bridge construction. As such, the AASHTO Guide Specifications for Wind Loads During Construction (AASHTO 2017) provides a reduction factor R to the design wind speeds according to the expected construction duration, as shown in Table 2.1.

As mentioned above, the NHI-130102 uses the same design wind speed as the AASHTO's recent specification; however, it includes a directionality factor of 0.85 in the basic wind pressure expression shown in Equation 1. As a result, the effective design wind speed approximately corresponds to an MRI of 50 years and an LF of 1.4, whereas AASHTO's recent specifications consider an MRI of 100 years and an LF of 1.4 (AASHTO 2017, 2020). This difference also affects the wind speed reduction factor for different construction durations in the two specifications, as can be seen in Table 2.1.

2.2.4   *Exposure and elevation factor (K_z)*

The wind speed profile is affected by the topography and obstructions of the bridge's immediate surrounding area. ASCE 7 provides three wind exposure categories: B, C, and D for urban and suburban areas, open terrain, and sea surface, respectively, based on the corresponding ground surface roughness that controls the wind speed increase rate with height (see (ASCE/SEI 2022) for more details on this classification). As previously mentioned, the 3-sec gust basic wind speed provided by ASCE 7 maps is measured at a height of 33 ft above the ground in wind exposure category C. Thus, it is the role of the exposure and elevation factor K_z to adjust this basic design wind speed based on the bridge wind exposure category and height above the ground.

Table 2.1: Wind speed reduction factor

Construction Duration	AASHTO (AASHTO 2017)	NHI-130102 (NHI 2015)
0-6 weeks	0.65	0.65
6 weeks to 1 year	0.73	0.75
1-2 years	0.75	0.80
2-3 years	0.77	0.85
3-5 years	0.84	0.85

AASHTO specifications (AASHTO 2017, 2020) adopt the logarithmic law to describe the wind speed profile, and thus provide the following expressions for $K_z(B)$, $K_z(C)$, and $K_z(D)$ in wind exposures B, C, and D, respectively. The lower bound shown in each expression below is the K_z computed at a minimum height (z_{min}) of 33 ft.

$$K_z(B) = \frac{\left[2.5 \ln\left(\frac{z}{0.9834}\right)+6.87\right]^2}{345.6} \geq 0.71 \tag{2}$$

$$K_z(C) = \frac{\left[2.5 \ln\left(\frac{z}{0.0984}\right)+7.35\right]^2}{478.4} \geq 1.00 \tag{3}$$

$$K_z(D) = \frac{\left[2.5 \ln\left(\frac{z}{0.0164}\right)+7.65\right]^2}{616.1} \geq 1.15 \tag{4}$$

In contrast, the NHI-130102 considers the wind speed profile power law to calculate K_z, which is originally adopted from ASCE 7-10 (ASCE/SEI 2010), as follows:

$$K_z = 2.01 \left(\frac{z}{z_g}\right)^{2/\alpha}, \tag{5}$$

where z_g is a gradient height, above which the mean wind speed and consequently K_z are assumed to be constant. ASCE 7-10 (ASCE/SEI 2010) provides values for the power law parameters: α, z_g, and z_{min}, as shown in Table 2.2. ASCE 7-22 (ASCE/SEI 2022) provided different values for the parameters in Equation 5; however, they only result in a slight difference in the computed K_z.

Figure 2.2 shows the exposure and elevation factor computed in wind exposure category C according to the logarithmic and power laws. As can be seen, there is only a significant difference for low heights, which is mainly a result of the different minimum heights (z_{min}), as shown above. The wind pressure profiles are expected to be similar to the ones shown in Figure 2.2, given the discussed role of the exposure and elevation factor.

Table 2.2: Power law parameters (ASCE/SEI 2010)

Construction	α	z_g (ft)	z_{min} (ft)
B	7.0	1,200	30
C	9.5	900	15
D	11.5	700	7
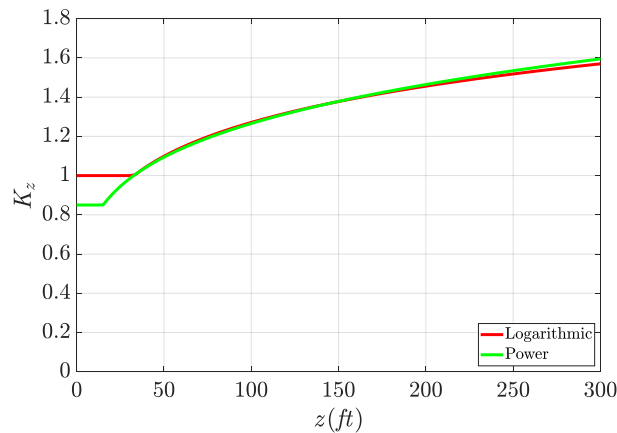
Figure 2.2: A comparison between the exposure and elevation factor computed in Wind Exposure category C according to the logarithmic and power laws.

2.2.5   Gust factor (G)

The gust factor G accounts for the distribution of gust wind over the bridge and the related dynamic effects. Wassef and Raggett (2014) performed a series of time-domain high-fidelity numerical simulations for wind effects on bridges with different spans to estimate this factor. Consequently, they recommended a gust factor of 1.0 for both constructed bridges and bridge superstructures during construction. Furthermore, they also found that bridges with a span of 203 ft, or less, are likely to be fully engulfed by a 3-sec gust wind speed, which supports the use of a gust factor of 1.0. The NHI-130102 however uses a gust factor of 0.85 (NHI 2015).

2.2.6   Drag coefficient (C_D)

The drag coefficient, C_D, is a dimensionless quantity, to consider the related aerodynamic characteristics of the studied object. For bridges under construction, there is interest in studying the stability of single girders as well as systems of girders before placing the deck. The bridge response to wind loads prior to the placement of the deck is significantly different from that of a fully constructed bridge since the deck changes the flow of wind around the girders, thus affecting the generated wind pressure on each girder. Consolazio et al. (2013) provided a detailed literature review on the drag coefficient for single I-girders, and they found that up to the time of their study,

wind tunnel studies were performed only for symmetric I-shapes girders with web depth-to-flange width ratios less than approximately 2:1. However, most steel I-girders used in long-span bridges have a web depth-to-flange width ratio greater than 2:1. Consequently, they performed wind tunnel tests for two plate girders having symmetric cross-sections with web depth-to-flange width ratios of 3:1 and 6:1. The former had an 8-ft deep web and 2′-8″ wide flanges, while the latter had the same web depth and flanges one-half as wide as the other plate girder (1′-4″). These wind tunnels tests ultimately resulted in a drag coefficient around 2.2 for the two studied sections, or, more conservatively, an effective drag coefficient, $C_{D_{eff}}$, approximately equal to 2.5, to account for any potential torque effects.

In addition, Consolazio et al. (2013) investigated the shielding effect in multi-girder bridge systems for various girder cross-sections and different girder spacings. This investigation was performed through numerous wind tunnel tests for systems consisting of 5 and 10 girders. For the I-girder bridge systems of relevance to the current study, Consolazio et al. (2013) identified multiple shielding trends. Specifically, an interesting finding was the negative drag on the first, second, and possibly the third shielded girders. As a result, Consolazio et al. (2013) proposed a conservative drag coefficient distribution model for I-girder bridge systems during construction, that is shown in Figure 2.3(a). As can be seen from this illustration, the first shielded girder does not have any applied wind load, whereas each subsequent shielded girder has half of the base drag coefficient C_D of the windward girder. This base drag coefficient shall be used as the drag coefficient for a single I-girder.

Based on the findings of Consolazio et al. (2013), the AASHTO Guide Specifications for Wind Loads During Construction (AASHTO 2017) provided a drag coefficient distribution model for different ratios of girder spacing to girder depth (S/D). Regardless of the S/D ratio, the windward girder is consistently subjected to the base drag coefficient, and the second girder in the system does not experience any wind pressure due to the significant shielding effect provided by the windward girder. As depicted in Figure 2.3(a), the distribution model for S/D ratios greater than 3 incorporates a drag coefficient reduction factor of 0.5 for the third and subsequent girders, the same as the drag coefficient distribution model recommended by Consolazio et al. (2013). However, for S/D less than or equal to 3, the shielding effect becomes more pronounced and a reduction factor of 0.25 is specifically applied to the third, fourth, and fifth girders, as illustrated in Figure 2.3(b). Noting that the sixth girder and any girders thereafter maintain a reduction factor of 0.5, regardless of the S/D ratio.

The targeted construction phase in this project is the completely erected steel superstructure with diaphragms installed but prior to the placement of the deck. Thus, the global stability of the completely erected steel superstructure is the main interest of the current study. By assigning a conservative drag coefficient for each component, as shown in Figure 2.3, the total estimated drag force on the system can be excessively conservative Consolazio et al. (2013).
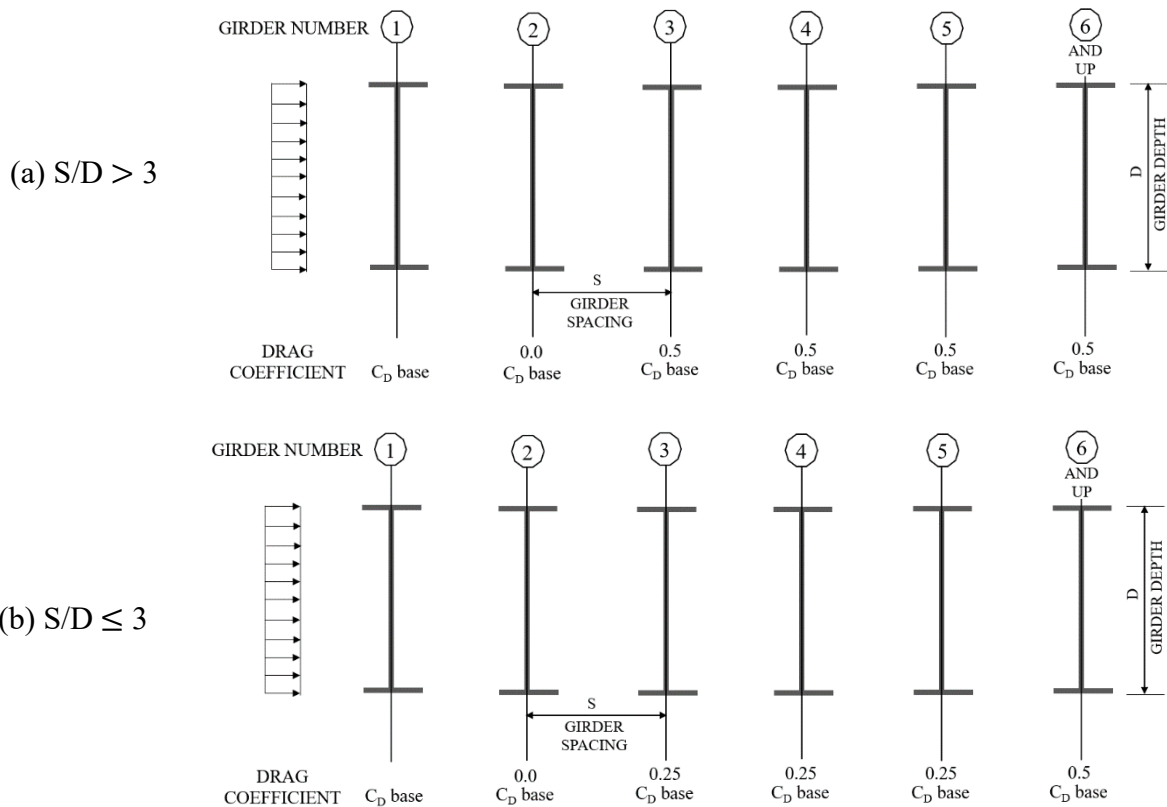
Figure 2.3: Drag coefficient (C_D) distribution model: (a) for ratios of girders spacing to girder depth (S/D) greater than 3, and (b) for S/D less than or equal to 3 (AASHTO 2017).

In this case, a reduction factor can be then introduced to the summation of the drag coefficients of each individual girder in order to compute a more reasonable system drag coefficient. Consolazio et al. (2013) proposed a reduction factor dependent on the number of girders in the system and the total unshielded system area. This reduction factor is approximately 0.5 for systems with 4 girders, or more. Nonetheless, the AASHTO Guide Specifications for Wind Loads During Construction (AASHTO 2017) states that to determine the total wind load on the superstructure at any stage of construction, the sum of the drag coefficients from all erected girders shall be considered as the system drag coefficient without any reduction factor, which is adopted in this study.

The NHI-130102, which is the reference for PennDOT wind loading on bridges during construction (PennDOT 2019a), adopts an expression for the drag coefficient C_D as a function of S/D as follows (NHI 2015):

$$C_D = 2(1 + 0.05(S/D)) \tag{6}$$

where $C_{D\,min} = 2.2$, and $C_{D\,max} = 4.0$. The wind pressure computed according to NHI-130102 is only applied on the windward girder according to (NHI 2015).

Table 2.3: PennDOT wind pressure for bridges during construction in psf (PennDOT 2019a).

Construction Duration	0-6 weeks		6 weeks- 1 Year		1-2 Years	
Superstructure Height Above Ground Level (ft)	S/D ≤ 2	2<S/D ≤ 4	S/D ≤ 2	2<S/D ≤ 4	S/D ≤ 2	2<S/D ≤ 4
0-15	19	21	26	28	29	32
20	20	22	27	30	31	34
25	21	23	28	31	32	35
30	22	24	30	32	34	37
40	24	26	31	34	36	39
50	25	27	33	36	38	41
60	26	28	34	37	39	42
70	27	29	35	39	40	44
80	28	30	37	40	42	45
90	28	31	38	41	43	47
100	29	31	38	42	43	47
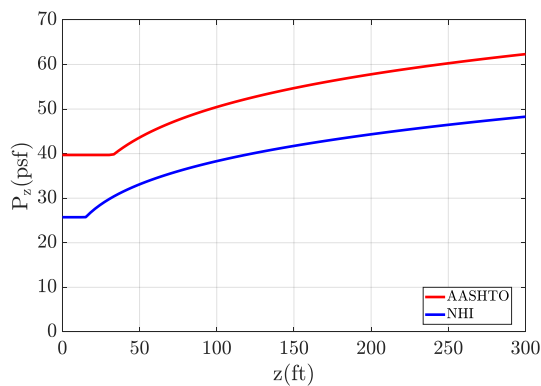
Figure 2.4: Base wind pressure for the illustrative example, computed according to AASHTO Guide Specifications for Wind Loads During Construction (AASHTO 2017) and NHI-130102.

2.2.7 PennDOT wind loading procedures

PennDOT Bridge Standard BD-620M considers the NHI-130102, discussed in the previous subsections, as a reference for the wind loading, including C_D shown in Equation 6. BD-620M provides a table for computed wind pressure according to NHI-130102 for bridges located in areas of wind exposure C, as depicted in Table 2.3 for convenience. As can be seen in Table 2.3, this table considers different superstructure elevation, construction duration, and different girder spacing to girder depth ratios. It is recommended that for bridges over traffic, this reported wind pressure should be increased by 5 psf. For bridges in a wind exposure category other than C, the PennDOT Bridge Standard BD-620M (PennDOT 2019a) requires adjusting the wind pressure according to the NHI-130102 procedure.

In contrast, BD-620M deviates from the NHI-130102 procedure by adopting for all bridges, regardless their S/D ratios, the drag coefficient distribution model provided by (AASHTO 2017) for S/D greater than 3, as seen in Figure 2.3(a). Consequently, the base wind pressure is computed based on NHI-130102 procedure, and it is then applied on each individual girder with the same reduction factors shown in Figure 2.3(a). An illustrative example is shown in the following subsection.

2.2.8 Illustrative example of wind pressure calculations on girder systems

The wind pressure during construction on a girder system consisting of four main girders, assuming that it is located in wind exposure C, the construction duration is 6 weeks to 1 year, the bridge deck level is 33 ft, and S/D = 2.0, is computed step by step in this section for illustration. First, the base wind pressure is determined according to (AASHTO 2017) and the wind pressure applied on the windward girder based on NHI-130102 (NHI 2015) as follows:

For (AASHTO 2017):

- Design wind speed = 115 mph (the map in Figure 2.1)
- Wind speed reduction factor = 0.73 (Table 2.1)
- Exposure and elevation factor = 1.0 (Equation 3)
- Gust factor = 1.0
- Base drag coefficient = 2.2
- Base wind pressure = $2.56 * 10^{-3} * (115)^2 * (0.73)^2 * 1.0 * 1.0 * 2.2 = 39.69$ psf

For NHI-130102 (NHI 2015):

- Design wind speed = 115 mph (the map in Figure 2.1)
- Wind speed reduction factor = 0.75 (Table 2.1)
- Exposure and elevation factor = 1.0 (Equation 5)
- Gust factor = 0.85
- Base drag coefficient = 2.2 (Equation 6)
- Directionality factor = 0.85

- Wind pressure $= 2.56 * 10^{-3} * (115)^2 * (0.75)^2 * 1.0 * 0.85 * 0.85 * 2.2 = 30.27$ psf

As can clearly be seen from the above calculations, the NHI-130102 (NHI 2015) underestimates in comparison to AASHTO the base wind pressure by 0.72 (0.85*0.85 (gust factor * directionality factor)), which should be the case for all heights, as shown in Figure 2.4. Now considering the wind pressure on the girder system, NHI-130102 (NHI 2015) only applies the computed wind pressure (30.3 psf) on the windward girder, whereas (AASHTO 2017) applies 39.7, 0, 9.9, and 9.9 psf on the facial, second, third, and fourth girder, respectively, which makes a significant difference in the total wind load applied on the girder system.

However, the PennDOT BD-620M adopts the conservative AASHTO drag coefficient distribution model, as mentioned previously, resulting in applying wind pressure of 30.3, 0, 15.1, and 15.1 psf on the windward, second, third, and fourth girder, respectively, thus being more conservative than its reference, i.e., NHI-130102 (NHI 2015).

2.3 PennDOT Lateral Stability Bracing

In this section, the horizontal bracing design criteria provided in the PennDOT Bridge Standard BD-620M (PennDOT 2019a) for steel girder bridges before deck completion, as also adopted in PennDOT Design Manual Part 4 (DM-4) (PennDOT 2019b), are summarized for the benefit of the discussion on structural modeling. These criteria are based on a defined permissible lateral displacement of L/150, where L is the girder span. This limit appears primarily based on engineering judgment and experience, as a single specific basis for L/150 is not provided in BD-620M/DM-4, or other related literature or specifications discussing lateral displacement limits. Based on the L/150 limit state and structural analysis, BD-620M/DM-4 provides various horizontal lateral bracing guidelines. These guidelines are summarized as follows (PennDOT 2019a):

a) For bridges with spans greater than 300 ft, lateral bracing is required to aid in the bridge construction, and it should also be designed to resist wind loads.
b) For bridges with spans between 200 ft and 300 ft, lateral bracing might be required in order to satisfy the L/150 lateral displacement limit.
c) For shorter girder spans, with a ratio of girder spacing over girder depth less than or equal to 2 and a bridge cross-section with 4 or more girders, the girders shall be designed to resist wind loads and satisfy the lateral displacement limit without any lateral bracing. This is also recommended by the Associated Pennsylvania Constructors (APC) Bridge Committee (PennDOT 2019a).

The PennDOT Bridge Standard BD-620M (PennDOT 2019a) also indicates that for straight, bridges with a skew angle of 90 degrees, that is no skew, this bracing should be designed to only assist in carrying the wind loads and not to participate in carrying primary structure forces. Bracing connections should be thus designed for wind forces only.
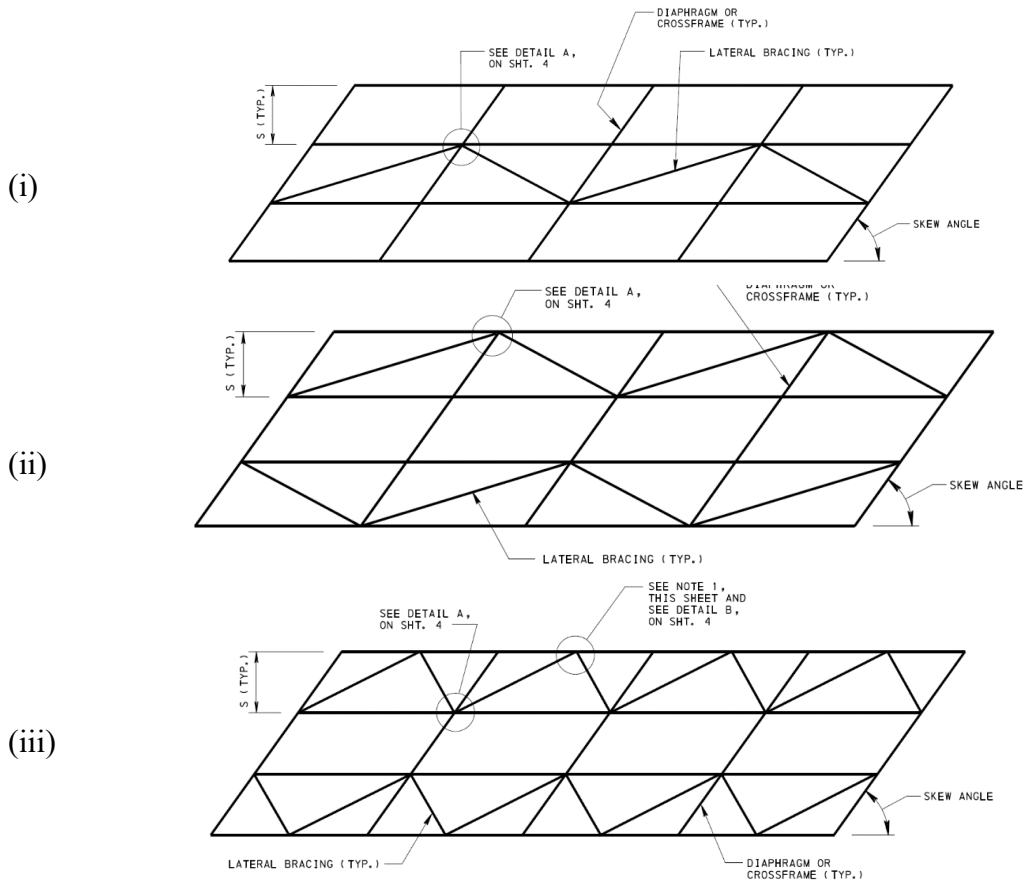
Figure 2.5: PennDOT lateral bracing recommended arrangements (PennDOT 2019a).

Although multiple configurations for the bracing connections are provided in the PennDOT Bridge Standard BD-620M, the preference is for attaching the brace members to the bottom flanges (PennDOT 2019a). Furthermore, PennDOT Bridge Standard BD-620M provides three recommended lateral bracing arrangements, as shown in Figure 2.5. While the bracing members are located in the middle bay of the bridge in Figure 2.5(i), they can also be arranged in the two bays adjacent to the middle bay, as shown in Figures 2.5(ii) and 2.5(iii). Since the lateral bracing arrangement shown in Figure 2.5(iii) is for skewed bridges, only arrangements shown in Figures 2.5(i) and 2.5(ii) is considered in this study, and they will be referred to as arrangement (a) and arrangement (b), respectively, hereafter. The PennDOT Bridge Standard BD-620M also recommends modeling the connections between the cross-frames and main girders as pinned connections in the plane of the girder.

Chapter 3 Structural Modeling

3.1 Introduction

In this chapter, the details of the structural modeling are provided, by showing the considered structural elements, supports, and connections, in addition to the structural analysis procedures. A case study bridge girder system is analyzed, to provide an example of wind loading and structural modeling and analysis, and importantly to verify the considered structural modeling and analysis procedures. Additional investigations are then discussed to explore the effect of rigid and partially fixed transverse diaphragm connections, as well as variations in the diaphragms' and braces' cross-section size, on the lateral displacement of girder systems. The impact of the uplift wind forces on system demands is also examined.

3.2 Structural Modeling

This report section describes the 2-dimensional (2D) finite element (FE) structural models developed to compute the lateral displacement due to wind loads. The FE models are analyzed using SAP2000 (CSI 2021). All girders and cross-girders are modeled as beam elements, while the lateral braces are modeled as truss elements and only axial deformations/forces are considered.

All external supports to the girder system are modeled as pins, that is translation is restrained while rotation is permitted. The connections between the cross-frames and main girders are modeled as pinned connections in the plane of the girder, as recommended in PennDOT Bridge Standard BD-620M. Consequently, the cross-frames are not expected to contribute significantly to the girder system's lateral stiffness; instead the cross-frames assist in maintaining the compatibility of lateral displacements between two adjacent girders. Furthermore, given that the connections between the cross-frames and main girders are pinned in the plane of the girder, they distribute the wind loads on all girders in the system. This point is discussed in more detail in later sections.

Since the wind pressure is assumed to be uniformly distributed along the depth and perpendicular to the side of the main girders, it is multiplied by the girder's total depth and applied as a lateral uniform line load at the girder centerline on the beam elements. It should be noted that, following convention, there is no lateral pressure applied on the cross-frames or the bracing elements. In the next subsection, a case study bridge is described and used to illustrate the details of the structural modeling just discussed.

3.2.1 Case study

A 3-span steel girder system is considered for this case study with span lengths of 250, 320, and 250 ft. The girder system consists of 4 main girders which are symmetric steel I-sections, spaced at 12 ft on center. The web and flange dimensions are 120 in deep x 0.75 in thick, and 22 in wide x 2 in thick, respectively. The resulting cross-section moments of inertia are $I_x = 435,000$ in^4, and $I_y = 3,550$ in^4, whereby the subscript x denotes the strong axis. It should be noted that I_y is the

moment of inertia of importance here since it contributes to the lateral stiffness of the system girder. The cross-frames are spaced at 25 ft along the length of the exterior spans and at 20 ft along the length of the middle span. The cross-frames are assumed to be symmetric steel I-sections with web and flange dimensions of 37.5 in deep x 0.5 in thick, and 15 in wide x 1.25 in thick, respectively. Utilizing this relatively large cross-section aims to reduce, to the extent possible, relative displacements between main girders under wind loading, thereby facilitating a more direct comparison between parametric cases in relation to the girder system lateral displacement. The sensitivity of lateral displacements to the transverse diaphragm's cross-section stiffness is investigated in detail in Subsection 3.3.2. The case study steel girder system is assumed to be in the wind exposure category C. The construction duration for this case study is assumed to be between 6 weeks to 1 year.

Three different cases are modeled with respect to lateral bracing: (i) without lateral bracing, (ii) with lateral bracing arrangement (a) as shown in Figure 2.5(i), and (3) with lateral bracing arrangement (b) as shown in Figure 2.5(ii). The cross-section of the bracing members is assumed to be 2L10 in x 10 in x ¾ in x ¾ in. Isometric views of 2D structural models developed in SAP 2000 are shown in Figure 3.1, where (i), (ii), and (iii) show the unbraced girder system, a braced girder system with bracing arrangement (a), a braced girder system with bracing arrangement (b), respectively. As discussed previously, the connections between the cross-frames and main girders are modeled as pinned in the plane of the girder system, so that there is no bending moment in these connections due to wind loads.

The wind loads are evaluated as discussed in Section 2.2, considering that the deck level is assumed to be 33 ft above the ground level. As per AASHTO, the wind loads applied on the windward, third and fourth girder are 410, 102, and 102 lb/ft, respectively. These values are computed by multiplying the wind pressure on each girder with the total height of the girder (10.33 ft). Given that the case study shares the same wind loading parameters with the illustrative example in Subsection 2.2.8, there was no need to recompute the wind pressure. Similarly, according now to PennDOT Standard BD-620M, these loads should be 312, 156, and 156 lb/ft, on the windward, third and fourth girders, respectively. Figure 3.2 shows the lateral displacement shapes for the three modeling cases shown in Figure 3.1.

(i)

(ii)

(iii)
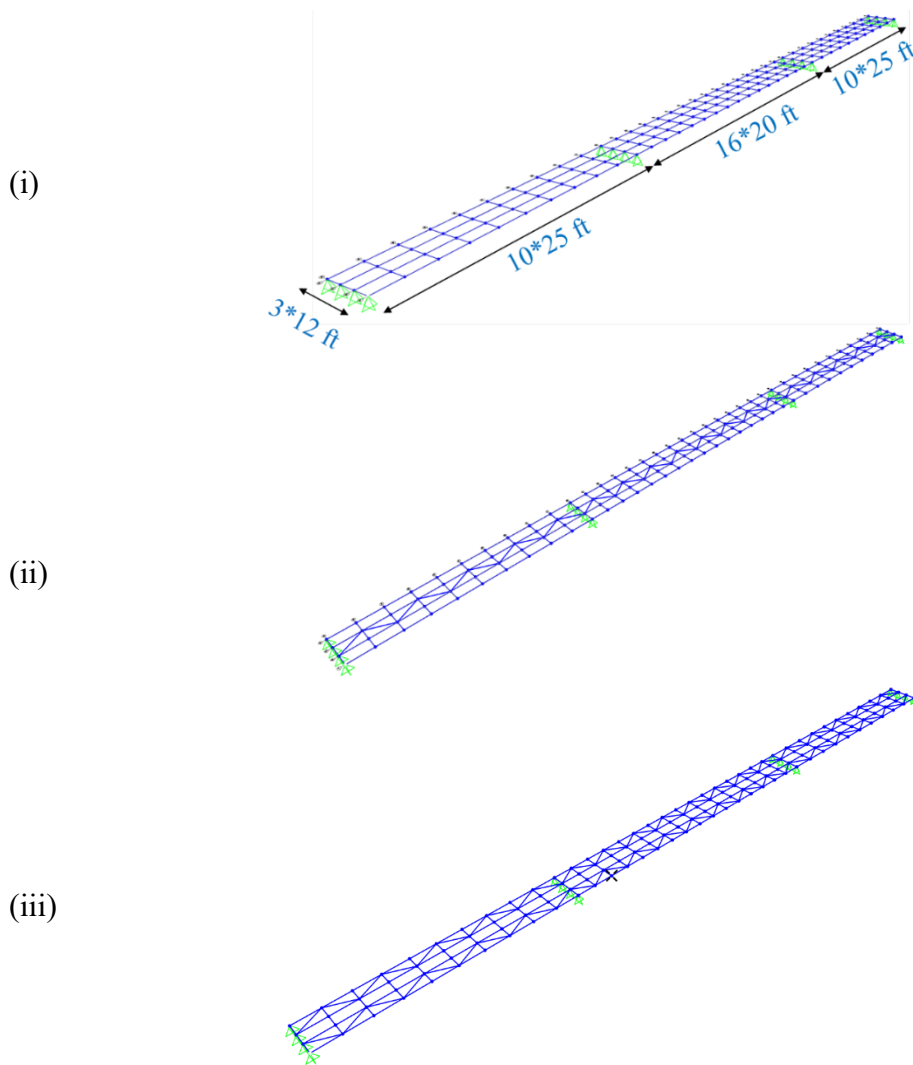
Figure 3.1: Isometric view of 2D structural models: (i) without lateral bracing, (ii) with lateral bracing arrangement (a), and (iii) with lateral bracing arrangement (b). All model connections between the main girders elements and the cross-frames elements are pinned, and all braces are modeled as truss elements.

(i)

(ii)

(iii)
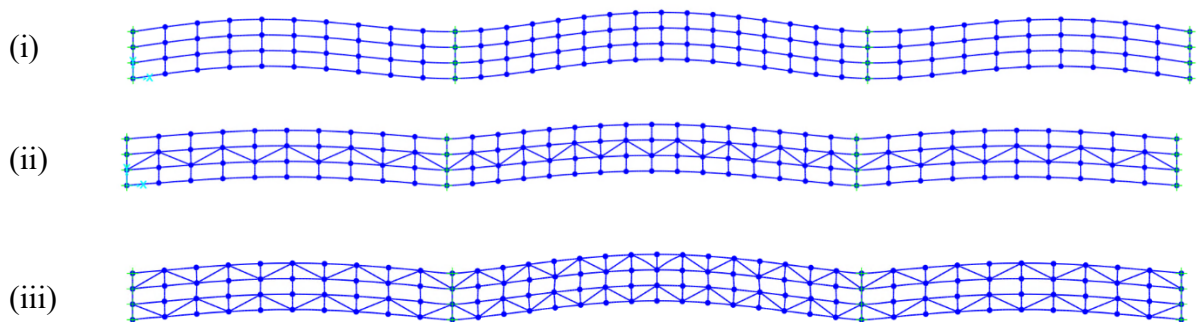
Figure 3.2: The lateral displacement shapes in plan view: (i) without lateral bracing, (ii) the braced model shown in Figure 3.1(ii), and (iii) the braced model shown in Figure 3.1(iii). All model connections between the main girder elements and the cross-frame elements are pinned, and all braces are modeled as truss elements.

Table 3.1: Maximum lateral displacement from SAP2000 for the case study (ft). The numbers written in blue font violate the permissible limit (L/150).

Structural System	L/150	AASHTO	BD-620M	Diff. % *
Without lateral bracing (Figure 3.1(i))	2.13	6.538	6.644	1.60
The braced model (Figure 3.1(ii))	2.13	0.086	0.087	1.57
The braced model (Figure 3.1(iii))	2.13	0.043	0.044	1.47

* Diff. % is computed by dividing the displacement difference (BD-620M – AASHTO) by the BD-620M displacement.

The maximum lateral displacements under the stated wind loads are provided in Table 3.1. To provide a quantitative comparison between the outcomes of the BD-620M and AASHTO procedures, the percent difference in the resulting maximum lateral displacements, referred to as Diff. %, is reported in Table 3.1 and all subsequent tables. This percentage is computed by dividing the displacement difference (BD-620M – AASHTO) by the BD-620M displacement. It should be noted that the difference percentage is computed with displacement values expressed to a higher decimal precision than those reported in the tables. For example, in the case of the braced system shown in Figure 3.1(ii), the difference percentage is calculated using displacement values of 0.085761 ft and 0.087129 ft, whereas the values reported in Table 3.1 are 0.086 ft and 0.087 ft accordingly. Comparing the maximum lateral displacement for the case without lateral bracing in Table 3.1 to the lateral displacement limit provided in PennDOT BD-620M (span length/150 = 320/150 = 2.13 ft), it is evident that the case without lateral bracing significantly violates the lateral displacement limit.

3.2.2 Model verification

3.2.2.1 Modeling approach verification

This first check is done in order to verify that the cross-frames, with their modeled pin connections, assist in creating a diaphragm mode to distribute the wind loads uniformly on all girders. In essence, the cross frames hence mainly serve to constrain each girder to the others. To verify this assertion, the unbraced girder system, shown in Figure 3.1(i), is modeled as a single girder with the average value of the girder system wind load applied, e.g., for AASHTO wind loads, the average is (410+102+102)/4≈154 lb/ft. Analyzing this single 3-span girder using SAP 2000, the maximum lateral displacement values in the AASHTO and BD-620M wind load cases are 6.534 and 6.641 ft, respectively.

Table 3.2: Maximum lateral displacement computed in model verification studies (ft).

Structural System	AASHTO	BD-620M	Diff. % *
2D FE model - Unbraced girder system (Figure 3.1(i))	6.538	6.644	1.60
2D FE model - 3-span single girder	6.534	6.641	1.60
Analytical - 3-span single girder	6.556	6.648	1.38
Analytical - Middle span with pin-pin boundary conditions	29.314	29.792	1.60
Analytical - Middle span with fixed-fixed boundary conditions	5.863	5.958	1.60

* Diff. % is computed by dividing the displacement difference (BD-620M – AASHTO) by the BD-620M displacement.

These values, which are also reported in the second row of Table 3.2, are approximately the same as those obtained for the unbraced girder system, as reported in the first row of Table 3.2, which supports the prior assertion. This result indicates that insights on the 2D FE model for the unbraced girder system can be also obtained by analyzing a 2D model of a single girder.

3.2.2.2 Model lateral displacement verification

The lateral displacement results of the 2D FE model are also verified for the original unbraced girder system model (S/D=1.16) by hand calculations, based now on the described 3-span beam mentioned above and two bounding cases based on single-span beams (i.e., the exact lateral displacement is not approximated in these bounding cases, rather its value is verified only in a bounded sense): (a) a pin-pin single-span beam, and (b) a fixed-fixed beam. For each case of the three analytical cases mentioned above the cross-section of the beam is the same as the main girder in the case study bridge.

The supports and span lengths of the 3-span beam are the same as the case study bridge, whereas the beam length for the two bounding analyses is equal to the middle span length (320 ft) in the case study bridge. All cases are subjected to the same average wind load computed in the case of the 3-span beam discussed above, i.e., 154 lb/ft for AASHTO, and 156 lb/ft for BD-620M. The resulting maximum lateral displacement for the pin-pin single-span beam, that is considering only the middle span, provides only an *upper bound* of the actual bridge lateral displacement, whereas the fixed-fixed beam accordingly provides a *lower bound* for the maximum bridge lateral displacement. Hereafter, based on the explanation above, the first, and second bounding cases will be called the middle span with pin-pin boundary conditions, and the middle span with fixed-fixed boundary conditions cases, respectively.

The analytical results for the 3-span beam case are obtained by using the method of the three-moment equation to compute the moments, and the conjugate beam method for evaluating the lateral displacement. The modulus of elasticity and the moment of inertia are $29*10^6$ psi, and $3,550$ in^4, respectively. The maximum lateral displacement for this case is reported in Table 3.2.

For the two bounding cases, the maximum lateral displacement in both cases is computed according to closed-form expressions, as follows (Hibbeler 2017):

- Bounding case 1: Middle span with pin-pin boundary conditions:

  lateral displacement $= \dfrac{5qL^4}{384EI}$

- Bounding case 2: Middle span with fixed-fixed boundary conditions:

  lateral displacement $= \dfrac{qL^4}{384EI}$

where q is the uniform wind load, L is the beam length, $E = 29*10^6$ psi is the modulus of elasticity, and $I = 3,550$ in^4 is the moment of inertia. The resulting lateral displacements are provided in Table 3.2. From the results presented in Table 3.2, the lateral displacement resulting in the original 2D FE model of unbraced girder system is approximately similar to the one analytically obtained for the 3-span beam case and slightly higher than the lower bound provided by the case of middle span with fixed-fixed boundary conditions, further verifying the developed 2D SAP2000 model for this study.

3.3 Additional Investigations

3.3.1 *Rigid and partially fixed connection*

The effect of rigid and partially fixed transverse diaphragm connections on lateral displacement is investigated and reported in this section. The case study bridge, previously described, serves as the basis for this investigation where the fixity of connection between the cross-frames and main girders is varied to determine the effect on the girder system (without braces) lateral displacement. Four cases are considered, comprising pinned connections, partially fixed connections with 50% of the rotational stiffness of the fixed connections, fixed connections, and fixed connections with the stiffness of the cross-frames having 50% of the original cross-frames' stiffness. The results of this investigation are summarized in Table 3.3. These results demonstrate that the lateral displacement of the girder systems is highly sensitive to the degree of connection fixity. This sensitivity is also evident even when less stiff cross-frames are employed. The lateral displacement limit for the case study bridge is 2.13 ft (span length /150) according to the BD-620M guidelines.

As seen in Table 3.3, for the case study bridge with the pinned connections, which is the recommended modeling approach in BD-620M, the lateral displacements significantly exceed the limit. Comparing the lateral displacements for all mentioned cases, as seen in Table 3.3, reveals that the current BD-620M pinned connections recommendation is conservative.

Table 3.3: Maximum lateral displacement for the unbraced girder system from SAP2000 for the case study (ft). The numbers written in blue font violate the permissible limit (L/150).

Structural System	L/150	AASHTO	BD-620M	Diff. % *
Pinned connections	2.13	6.538	6.644	1.60
Pinned connections (Reduced stiffness (50%) for the cross-frames)	2.13	6.538	6.644	1.60
Partially fixed connections (50% of the rotational stiffness of the connections)	2.13	0.924	0.939	1.61
Fixed connections	2.13	0.417	0.424	1.61
Fixed connections (Reduced stiffness (50%) for the cross-frames)	2.13	0.692	0.703	1.60

* Diff. % is computed by dividing the displacement difference (BD-620M – AASHTO) by the BD-620M displacement.

3.3.2   Variations in the cross-section size of transverse diaphragms

In this section, the impact of the cross-section size of the transverse diaphragms on the lateral displacement is investigated, again taking the case study bridge as the basis. Two cross-frame sections are utilized in this study. The first, as utilized in the case study bridge, is a symmetric steel I-section with web and flange dimensions of 37.5 in deep x 0.5 in thick, and 15 in wide x 1.25 in thick, respectively. The second section is defined as a section having 50% of the original section's axial and flexural stiffnesses. Furthermore, two cases are considered with respect to the fixity of these cross-frames: *(i)* pinned connections, and *(ii)* fixed connections.

The results of this investigation are summarized in Table 3.3. These results demonstrate that the lateral displacement of the girder systems is largely insensitive to the transverse diaphragm section stiffness for pinned connections, whereas a high sensitivity is instead observed to the cross frames section size in the case of fixed connections. Since pinned connections are recommended by PennDOT BD-620M (PennDOT 2019a) for the studied girder systems, the original cross-section is deemed suitable for all subsequent models analyzed in this study, as there is no appreciable difference in transverse displacements for the different cross-frame stiffnesses.

Table 3.4: Maximum lateral displacement for the braced system from SAP2000 for the case study (ft).

Bracing members	Cross-section area (in²)	Bracing Arrangement	AASHTO (ft)	BD-620M (ft)	Diff. % *
2L10 in x 10 in x ¾ in x ¾ in	29	(a)	0.086	0.087	1.57
		(b)	0.043	0.044	1.47
C-channel 18 x 42.7	12.6	(a)	0.135	0.137	1.59
		(b)	0.069	0.070	1.62

* Diff. % is computed by dividing the displacement difference (BD-620M – AASHTO) by the BD-620M displacement.

Higher precision for the reported lateral displacements reveals a marginal effect of the cross-frame section size on the relative displacement between main girders. To summarize, the AASHTO's lateral displacements, in ft, on the same transverse axis at each main girder (G) are 6.53757 at G1, 6.53753 at G2, 6.53752 at G3, and 6.53751 at G4 for the original cross-section with pinned connections. Whereas for the 50% stiffness case, these displacements now become 6.53761 at G1, 6.53753 at G2, 6.53750 at G3, and 6.53749 at G4. It can be seen that less stiff cross-sections allow for a modest relative displacement between the main girders. However, compared to the overall lateral displacement of the girder system, these relative values are negligible.

3.3.3   Variations in the cross-section size of braces

This investigation examines the impact of the cross-section size of the braces on the lateral displacement, again taking the case study bridge as the basis. For this investigation, the considered brace sections are C-channel (C18X42.7) and double angle 2L10 in x 10 in x ¾ in x ¾ in, the latter being also employed in all braced girder systems studied in Section 3.2. Two different bracing arrangements are considered for this investigation, designated as arrangement (a) and arrangement (b), where the braces are placed in the middle bay and the two bays adjacent to the middle bay, respectively, in accordance with the guidelines outlined in PennDOT BD-620M (PennDOT 2019a). Table 3.4 summarizes the lateral displacement results for the C-channel and 2L10 in x 10 in x ¾ in x ¾ in braces, where it can be seen that the lateral displacements for the C-channel braces are larger than the double angle, yet, both are well below the lateral displacement limit of $L/150$.

3.3.4   Impact of uplift forces on system demands

In this section, the impact of the wind uplift forces on the girder system demands is investigated. The uplift wind pressure is typically calculated using an uplift coefficient, an approach that is analogous to the drag coefficient used for the drag forces. Upon conducting a comprehensive review of relevant codes and specifications, it was found that there are no recommendations for uplift coefficients for the studied girder systems prior to deck placement.
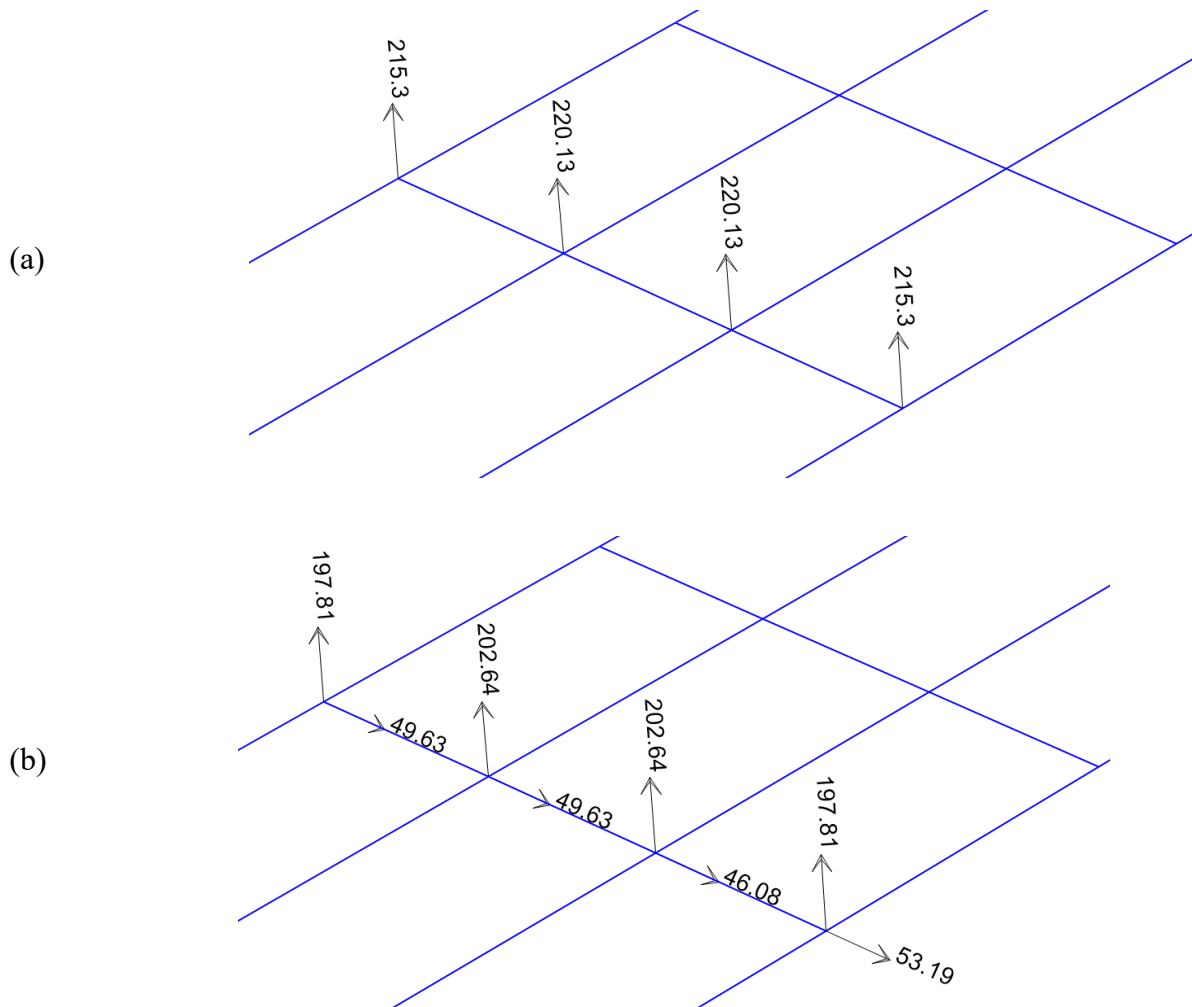
Figure 3.3: Reactions of internal supports of the case study bridge due to (a) the self-weight of the girder system, (b) a combination of the self-weight of the girder system, and PennDOT uplift and drag wind loads. The small differences in the vertical reactions between the two loading cases ensure that the girder system is not at risk of overturning as a result of vertical uplift wind forces.

The PennDOT Bridge Construction Standard BC-772M suggests an uplift wind pressure of 0.03 ksf to design temporary lateral stability bracing for single prestressed concrete beams (PennDOT 2010). This uplift wind load is adapted for the purpose of this study to be applicable to the studied girder systems. In lieu of specific guidance for girder systems, the uplift wind load for each girder is thus computed as the recommended wind pressure (0.03 ksf per BC-772M), however, it is multiplied by the full width of the girder's lower flange and applied as an upward line load on each girder.

The case study bridge is again employed as the basis for this investigation, whereby the uplift wind load has been computed as 0.03 ksf x 22 in (width of flange) = 0.06 kip/ft for each girder.

Analyzing the model of the unbraced girder system of the case study bridge revealed that these uplift forces have no discernible impact on the lateral displacement of the girder systems and the total uplift wind force is negligible in comparison to the self-weight of the girder system. This result is further supported by the inconsequential variations in the vertical reactions of supports, caused by the uplift wind load, as illustrated in Figure 3.3, thereby also indicating the girder system is not at risk of overturning as a result of vertical uplift wind forces.

These results are in agreement with research conducted by Consolazio et al. (2013). As previously discussed in Chapter 2, they extensively examined the impact of wind on various girder cross-sections using wind tunnel tests. The results of their study are reported in terms of drag and uplift coefficients. For the I-girder cross-sections of relevance to the current study, Consolazio et al. (2013) determined that the uplift coefficient is negligible, with a maximum magnitude of 0.05. Based on the results obtained from the above investigation and the conclusion of Consolazio et al. (2013), the uplift wind is not expected to control the stability of the studied straight girder systems with a 90-degree skew angle and has not been included in subsequent analyses.

Chapter 4 Parametric Study

4.1 Introduction

A parametric study is performed to further assess the PennDOT lateral bracing guidelines, considering all relevant parameters involved in wind loading, structural modeling, and analysis. Numerous girder systems with different parameter values are analyzed, with a particular emphasis on comparing the lateral displacement of the girder systems against the permissible values outlined in PennDOT BD-620M (PennDOT 2019a). A comprehensive analysis of the parametric study results is also provided.

4.2 Parametric Study

The objective of the parametric study is to Comprehensively evaluate the lateral bracing guidelines provided in PennDOT standard BD-620M (PennDOT 2019a), previously explained in Chapter 2. Herein, the design of the parametric study is outlined, followed by a presentation of the obtained results. An analysis of these results is also provided.

4.2.1 Parametric study design

To implement the parametric study, it is necessary to first identify the primary parameters involved in wind loading and structural modeling. These parameters can be listed as follows: (1) wind exposure category, (2) the level of the bridge deck, (3) the wind loading procedure, (4) the ratio between girders spacing to the depth of the girders (S/D), (5) the structural system of the girders, e.g., single span or multi-span, (6) the length of each span of the bridge, (7) the lateral bracing system, (8) the cross-section of the main girder and bracing members, and (9) the projected construction period of the bridge. Suggested representative values for each of the parameters numbered one through seven are shown in Table 4.1.

With respect to the cross-section of the main girders, it is postulated that the cross-section used for the case study bridge is sufficiently representative for the range of bridge configurations examined in this parametric study, specifically a symmetric steel I-section, with web and flange dimensions of 120 in deep x 0.75 in thick, and 22 in wide x 2 in thick, respectively. Consequently, the S/D ratios of 1.16, 2, and 3.5, as listed in Table 4.1, imply that the spacing of the main girders will be 12, 20.7, and 36 ft, respectively. While the main girder spacing of 12 ft is typical, it is understood that a girder spacing of 36 ft is theoretical, but it is included here to investigate the effect of having S/D greater than 3, see Section 2.1 for more details. An S/D greater than 3 is realistically possible if a smaller main girder's cross-section is used, which is shown through an example bridge in the following subsection.

Table 4.1: Parameters and values for the parametric study.

Parameter	Parameter values to be considered								
Wind exposure	B							C	
Bridge deck level (ft)	33							66	
Wind loading procedure	AASHTO							BD-620M	
Structural system	Single span							Multi-span	
Spans length (ft)	100	125	130	140	150	200	250	150 - 250 - 150	250 - 320 - 250
Girder spacing to girder depth (S/D)	1.16				2			3.5	
Lateral bracing system	Without lateral bracing				Arrangement (a)			Arrangement (b)	

Similarly, the cross-section of the cross-frames is considered the same as the case study bridge, that is a symmetric steel I-section with web and flange dimensions of 37.5 in deep x 0.5 in thick, and 15 in wide x 1.25 in thick, respectively. As previously discussed in Subsection 3.3.1, the lateral displacement of the girder systems is highly sensitive to the degree of fixity of the transverse diaphragm connections. Due to the complexities involved in determining the degree of partial fixity in practice, the parametric study considered two specific scenarios: (a) Pinned connections, as recommended by the PennDOT standard BD-620M (PennDOT 2019a), and (b) fixed connections.

Additionally, based on the relatively low sensitivity of lateral displacement to the cross-section size of braces, as discussed in Subsection 3.3.2, the braces are modeled as double angle 2L10 in x 10 in x ¾ in x ¾ in for all relevant cases in the parametric study. As listed in Table 4.1, two different bracing arrangements are considered for this study, designated as arrangement (a) and arrangement (b), where the braces are placed in the middle bay and the two bays adjacent to the middle bay, respectively, in accordance with the guidelines outlined in PennDOT BD-620M (PennDOT 2019a), see Figures 2.6(i) and 2.6(ii) for layouts of these two arrangements. According to the discussion presented in Chapter 2, the projected construction period of the bridges determines the reduction factor for the design wind speed. For the parametric study, a construction period spanning from 6 weeks to 1 year is considered suitable.

The combinations of the parameter values listed in Table 4.1 will form particular cases for the parametric study. For example, one combination can be a single-span bridge having a span length of 250 ft and an S/D ratio of 1.16, located in areas with wind exposure category C, with a deck placed at level 33 ft, and with bracing members having arrangement (a). Since considering wind exposure C always gives higher wind pressure than wind exposure B, only a few combinations

with wind exposure B are examined. More combinations of the more common parameter values are also studied, for example, a deck level of 33ft in comparison to the less common parameter values of 66 ft elevation.

4.2.2 *Parametric study results*

In accordance with the parametric study design previously discussed, 192 cases are formed for the examination of wind loads on the girder systems. These cases are subsequently modeled and analyzed according to the procedure outlined in Chapter 3, as described for the case study girder system. The results for these cases, presented in terms of the maximum lateral displacement of the girder system, are presented in Table 4.2. Additionally, for comparison purposes, the permissible lateral displacement specified by the PennDOT BD-620M for each girder system (span length (L) divided by 150, or L/150) is also reported. As previously mentioned, to provide a quantitative comparison between the outcomes of the BD-620M and AASHTO procedures, the percent difference in the resulting maximum lateral displacements, referred to as Diff. %, is reported in Table 4.2, and elsewhere. Again, this percentage is computed by dividing the displacement difference (BD-620M – AASHTO) by the BD-620M displacement. It should be noted that the difference percentage is computed with displacement values expressed to a higher decimal precision than those reported in the tables. For all cases presented in Table 4.2, only the more typical deck level of 33 ft and the common configuration of four main girders are considered.

From the results presented in Table 4.2, it is evident that the braced girder systems exhibit lateral displacements that are well below the permissible L/150 limit, emphasizing the effectiveness of lateral bracing in suppressing such displacement due to wind loads on girder systems. In contrast, the unbraced girder systems modeled with pinned transverse diaphragm connections, as recommended in BD-620M, have lateral displacements that in most cases exceed the allowable limit, except for the 100 ft, 125 ft and 130 ft single-span bridges. Considering the unbraced systems but with fixed cross-frame connections results in significantly lower lateral displacements in comparison to the pinned case, also illustrating the high sensitivity to the degree of fixity of the cross-frame connections by the substantial reductions in lateral displacements. Despite the fact that the fixed connections result in lateral displacements that are below the allowable limit, it is noted that achieving fixed connections might not be practical in most situations, due to the bridge design or construction procedures.

Table 4.2: Maximum lateral displacement for the cases examined in the parametric study (ft); the numbers written in blue font violate the permissible limit (L/150).

Bridge structure	Span length (ft)	S/D	L/150 (ft)	Without lateral bracing (Pinned connections) (ft)			Without lateral bracing (Fixed connections) (ft)			Lateral bracing in the middle bay (Arrangement a) (ft)			Lateral bracing as in Arrangement b (ft)		
				AASHTO	BD-620M	Diff. % *	AASHTO	BD-620M	Diff. % *	AASHTO	BD-620M	Diff. % *	AASHTO	BD-620M	Diff. % *
Single span	100	1.16	0.67	0.280	0.284	1.59	0.043	0.044	1.48	0.006	0.006	2.11	0.002	0.002	0.62
		3.5	0.67	0.373	0.306	-22.21	0.109	0.089	-22.21	0.004	0.003	-22.22	0.002	0.002	-22.27
	125	1.16	0.83	0.682	0.693	1.57	0.074	0.075	1.32	0.010	0.010	2.60	0.005	0.005	3.56
		3.5	0.83	0.911	0.746	-22.21	0.198	0.162	-22.21	0.006	0.005	-22.21	0.003	0.002	-22.27
	130	1.16	0.87	0.798	0.811	1.57	0.085	0.086	1.32	0.012	0.012	2.59	0.006	0.006	3.57
		3.5	0.87	1.066	0.872	-22.21	0.226	0.185	-22.21	0.006	0.005	-22.18	0.003	0.003	-22.15
	140	1.16	0.93	1.074	1.091	1.60	0.077	0.078	1.48	0.010	0.010	0.84	0.005	0.005	2.46
		3.5	0.93	1.434	1.173	-22.21	0.223	0.183	-22.21	0.007	0.006	-22.23	0.004	0.003	-22.21
	150	1.16	1.00	1.414	1.437	1.60	0.113	0.115	1.32	0.015	0.015	0.66	0.007	0.008	2.60
		3.5	1.00	1.889	1.546	-22.21	0.316	0.258	-22.21	0.008	0.006	-22.22	0.004	0.004	-22.24
	200	1.16	1.33	4.470	4.542	1.60	0.216	0.219	1.58	0.030	0.030	1.18	0.015	0.015	0.60
		3.5	1.33	5.969	4.885	-22.21	0.633	0.518	-22.21	0.015	0.012	-22.21	0.007	0.006	-22.23
	250	1.16	1.67	10.911	11.089	1.60	0.350	0.355	1.59	0.052	0.053	1.38	0.026	0.026	1.03
		3.5	1.67	14.572	11.924	-22.21	1.055	0.863	-22.21	0.023	0.019	-22.21	0.012	0.009	-22.22
Multi-span	150 - 250 -150	1.16	1.67	3.331	3.385	1.60	0.319	0.324	1.60	0.050	0.051	1.54	0.026	0.026	1.54
		3.5	1.67	4.448	3.640	-22.21	0.870	0.712	-22.21	0.023	0.018	-22.19	0.011	0.009	-22.16
	250 - 320 -250	1.16	2.13	6.538	6.644	1.60	0.417	0.424	1.61	0.086	0.087	1.57	0.043	0.044	1.47
		3.5	2.13	8.731	7.144	-22.21	1.223	1.001	-22.21	0.040	0.033	-22.21	0.020	0.017	-22.21

* Diff. % is computed by dividing the displacement difference (BD-620M – AASHTO) by the BD-620M displacement.

Again, from the results presented in Table 4.2, it is also observed that for S/D of 1.16, the PennDOT standard BD-620M wind loading procedure results in slightly higher lateral displacements compared to those based on the AASHTO procedure. In contrast, for the less common cases with S/D of 3.5, the AASHTO wind loads result in lateral displacement higher than those determined following the PennDOT standard. For S/D less than or equal to 3, since PennDOT BD-620M standard specifies a more conservative drag coefficient distribution model compared to AASHTO, this results in a larger lateral displacement for the PennDOT standard compared to AASHTO, when considering their entire process described in the two standards as outlined in this document. However, an opposite situation is observed for S/D ratios greater than 3 given that the PennDOT BD-620M standard generally provides lower wind pressure in comparison to the AASHTO procedure, as discussed in Chapter 2, while both AASHTO and PennDOT standard BD-620M utilize the same drag coefficient distribution model for S/D ratios greater than 3, shown in Figure 2.3(a). The aforementioned observation for S/D less than or equal to 3 is also dependent on the number of girders in the girder system, as further investigated in the following section.

Additionally, the influence of the wind exposure and deck level on lateral displacements is investigated. Various additional cases are accordingly analyzed, considering wind exposures B and C, and deck levels of 33 and 66 ft. The results, presented in Table 4.3, indicate that girder systems under wind exposure B always exhibit lower lateral displacements compared to wind exposure C cases, for equivalent deck heights. In contrast, elevated deck levels result in higher wind pressure, thus leading to higher lateral displacements.

As previously discussed, S/D ratios greater than 3, although less common, are plausible for main girders with shallower cross-sectional depths. For example, consider a modified version of the 125ft-single span bridge with main girders of symmetric steel I-section, with web and flange dimensions of 60 in deep x 0.75 in thick, and 22 in wide x 2 in thick, respectively, instead of the case study bridge's cross-section with a web depth of 120 in for the obtained results in Table 4.2. It is understood that these proportions of cross-sections are not typical, however, this example provides a data point for S/D ratio greater than 3 with a reasonable girder spacing. If, for instance, S/D ratios of 1.13, and 3.19 are now considered, the spacing of the main girders would be 6 and 17 ft, respectively, which falls within the plausible range of girder spacings. The maximum lateral displacements for these two S/D ratio cases described here are listed in Table 4.4 and, as expected, are fully consistent with the findings and patterns in Table 4.2.

Table 4.3: Maximum lateral displacement for various unbraced girder systems located in areas of different wind exposure categories and deck elevation levels (S/D = 1.16) (ft); the numbers written in blue font violate the permissible limit (L/150).

Bridge structure	Span length (ft)	Wind Exposure	Deck level (ft)	L/150 (ft)	Lateral displacement (ft)		
					AASHTO (ft)	BD-620M (ft)	Diff. % *
Single span	100	B	33	0.67	0.198	0.205	3.33
			66	0.67	0.246	0.249	1.45
		C	33	0.67	0.280	0.284	1.59
			66	0.67	0.328	0.330	0.68
	125	B	33	0.83	0.483	0.499	3.31
			66	0.83	0.600	0.609	1.43
		C	33	0.83	0.682	0.693	1.57
			66	0.83	0.800	0.806	0.66
	150	B	33	1.00	1.002	1.037	3.33
			66	1.00	1.244	1.262	1.46
		C	33	1.00	1.414	1.437	1.60
			66	1.00	1.659	1.670	0.69
Multi-span	250 - 320 -250	B	33	2.13	4.632	4.791	3.33
			66	2.13	5.750	5.835	1.46
		C	33	2.13	6.538	6.644	1.60
			66	2.13	7.666	7.719	0.69

* Diff. % is computed by dividing the displacement difference (BD-620M – AASHTO) by the BD-620M displacement.

Table 4.4: Maximum lateral displacement for unbraced girder systems of 125 ft-single span bridge with smaller main girders' cross sections and different S/D ratios (ft).

S/D	Girder spacing (ft)	L/150 (ft)	Lateral displacement (ft)		
			AASHTO (ft)	BD-620M (ft)	Diff. %*
1.13	6	0.83	0.352	0.358	1.58
3.19	17	0.83	0.470	0.385	-22.21

* Diff. % is computed by dividing the displacement difference (BD-620M – AASHTO) by the BD-620M displacement.

4.3 Discussion

As previously mentioned, for girder systems with S/D less than or equal to 3, the discrepancy between the lateral displacement resulting from AASHTO and PennDOT BD-620M standard is contingent upon the number of the main girders. The case study bridge and the 150-ft single span bridge, examined in the parametric study, served as a basis to investigate this point. Table 4.5 shows the maximum lateral displacement of the unbraced girder system for the case study bridge and the 150-ft single span bridge considering a varying number of main girders. It is observed that PennDOT standard results in lateral displacement estimation higher than the AASHTO wind loading procedure for the most typical cases, i.e., cases of girder systems with 4, 5 and 6 main girders. This finding also suggests that the PennDOT standard can yield slightly less conservative lateral displacement compared to AASHTO, for less typical cases with S/D less than or equal to 3. This is primarily due to the lower design wind pressure recommended by the PennDOT standard BD-620M in comparison to AASHTO.

A specific scenario for bridges under construction, but over traffic, is discussed here. As PennDOT BD-620M standard recommends an increase of 5 psf to the design wind pressure for such bridges, some cases, where BD-620M is less conservative in general settings than AASHTO are analyzed. These cases, accompanied by their maximum lateral displacements, are demonstrated in Table 4.6. As revealed by these results, for bridges over traffic and having S/D less than or equal to 3, the PennDOT BD-620M standard is more conservative than AASHTO, except for cases with 2 main girders. In contrast, for bridges over traffic and having S/D greater than 3, the PennDOT BD-620M standard is still slightly less conservative than AASHTO.

Table 4.5: Maximum lateral displacement for the unbraced girder system for the case study bridge and the 150 ft-single span bridge (S/D = 1.16) with a varying number of main girders (ft). The numbers written in blue font violate the permissible limit (L/150).

Number of main girders	Case study bridge				150 ft-single span bridge			
	L/150 (ft)	AASHTO (ft)	BD-620M (ft)	Diff. % *	L/150 (ft)	AASHTO (ft)	BD-620M (ft)	Diff. % *
2	2.13	8.731	6.644	-31.41	1.00	1.889	1.437	-31.41
3	2.13	7.269	6.644	-9.40	1.00	1.573	1.437	-9.40
4	2.13	6.538	6.644	1.60	1.00	1.414	1.437	1.60
5	2.13	6.099	6.644	8.20	1.00	1.319	1.437	8.20
6	2.13	6.538	6.644	1.60	1.00	1.414	1.437	1.60
7	2.13	6.851	6.644	-3.11	1.00	1.482	1.437	-3.12

* Diff. % is computed by dividing the displacement difference (BD-620M – AASHTO) by the BD-620M displacement.

Table 4.6: Maximum lateral displacement for various over traffic cases of the unbraced girder system of the case study bridge (ft); the numbers written in blue font violate the permissible limit (L/150).

Number of main girders	S/D	Over traffic	L/150 (ft)	Lateral displacement (ft)		
				AASHTO (ft)	BD-620M (ft)	Diff. % *
2	1.16	False	2.13	8.731	6.644	-31.41
		True	2.13	8.731	7.744	-12.74
3	1.16	False	2.13	7.269	6.644	-9.40
		True	2.13	7.269	7.744	6.14
7	1.16	False	2.13	6.851	6.644	-3.11
		True	2.13	6.851	7.744	11.54
4	3.5	False	2.13	8.731	7.144	-22.21
		True	2.13	8.731	8.246	-5.88

* Diff. % is computed by dividing the displacement difference (BD-620M – AASHTO) by the BD-620M displacement.

In relation to the presented results for bridges having span lengths of 200 ft or less, the current PennDOT standard BD-620M (PennDOT 2019a) states that for girder spans less than 200 ft, with a ratio of girder spacing over girder depth less than or equal to 2 and a bridge cross-section with 4 or more girders, the girders shall be designed to resist wind loads and satisfy the lateral displacement limit without any lateral bracing. However, the results of the parametric study show that, for single-span unbraced girder systems utilizing pinned connections and having span lengths of 140 ft or greater, in general, the lateral displacement values exceed the permissible $L/150$ displacement limit. This suggests that in order to satisfy the displacement limit, the weak axis moment of inertia of the main girder cross-sections need to be increased possibly significantly to be compliant without the addition of lateral braces. Thus, it might be more practical and require less material (steel) to also require and/or consider the option of lateral bracing in these cases.

In summary, for the more common cases of S/D less than or equal to 3 and 4-6 main girders, PennDOT BD-620M standard will result in higher lateral displacement values, when compared to the corresponding AASHTO values. Additionally, for bridges with span lengths of 140 ft or greater and without lateral bracing, the lateral displacements with wind pressures computed according to PennDOT BD-620M exceed the $L/150$ displacement limit.

Chapter 5 Summary, Conclusions, and Recommendations

5.1 Summary and Conclusions

This section first summarizes the performed assessment and evaluation for PennDOT's current specifications, outlined in the PennDOT Bridge Design Standard BD-620M (PennDOT 2019a), for wind loading on erected steel girder systems with diaphragms installed but prior to the placement of the deck. The wind loading assessment procedure in relevance to this study consists of two main stages: the estimation of the base wind pressure applied to the windward girder of the girder system, and the application of this base wind pressure to each one of the other girders with a specified reduction factor. Each stage is individually assessed, followed by a comprehensive evaluation of the entire PennDOT wind loading procedure.

In Chapter 2, it was discussed that the BD-620M standard generally recommends lower base wind pressure values compared to the AASHTO Guide Specifications for Wind Loads During Construction (AASHTO 2017). The BD-620M references the National Highway Institute (NHI) course number 130102 (NHI 2015) for its base wind pressure calculation, which considers various parameters, including the basic design wind speed, reduction factor to the design wind speed, exposure and elevation factor, gust effect factor, directionality factor, and drag coefficient. While both AASHTO and BD-620M use the same ASCE 7-10 design wind speed (ASCE/SEI 2010), there are discrepancies in other wind loading parameters, with the differences in the gust factor and directionality factor being the most notable. Specifically, the NHI-130102 recommends a gust factor of 0.85 and a directionality factor of 0.85, while AASHTO recommends a gust factor of 1.0 based on state-of-the-art research (Wassef and Raggett 2014) and does not include the directionality factor in its relevant procedure.

As a result, the base wind pressure values recommended by BD-620M are slightly lower, ranging from approximately 0.72 to 0.79 of the corresponding AASHTO values, depending on the girder spacing to girder depth (S/D) ratios. Both AASHTO and BD-620M use a drag coefficient of 2.2 when the S/D ratio is less than or equal to 2, resulting in a PennDOT base wind pressure value of around 0.72 of the AASHTO corresponding value. However, when the S/D ratio is between 2 and 4, PennDOT uses a more conservative drag coefficient of 2.4, resulting in a base wind pressure value of around 0.79 of the AASHTO corresponding value. It is worth noting that the ratios of 0.72 and 0.79 are approximate due to slight differences in the wind velocity reduction factor and the exposure and elevation factor between AASHTO and BD-620M. In fact, this minor difference in the exposure and elevation factor exists for bridge decks at elevations greater than 33ft, while for lower elevations AASHTO provides higher values for this factor, as depicted in Figure 2.2, thus making BD-620M comparatively less conservative than AASHTO. As a specific case, BD-620M recommends an increase of 5 psf in the base wind pressure for bridges over traffic.

Having examined the PennDOT base wind pressure of relevance, the distribution of wind pressure on each girder in the girder system is now being discussed to assess the complete PennDOT wind loading procedure. Due to wind shielding effects encountered in girder systems, extensively studied in (Consolazio et al. 2013), the AASHTO Guide Specifications for Wind Loads During Construction (AASHTO 2017) provided a drag coefficient distribution model for different ratios of girder spacing to girder depth (S/D). Regardless of the S/D ratio, the windward girder is consistently subjected to the base drag coefficient, and the second girder in the system does not experience any wind pressure due to the significant shielding effect provided by the windward girder. The distribution model for S/D ratios greater than 3 incorporates a drag coefficient reduction factor of 0.5 for the third and subsequent girders. However, for S/D less than 3, the shielding effect becomes more pronounced, and a reduction factor of 0.25 is specifically applied to the third, fourth, and fifth girders. Noting that the sixth girder and any girders thereafter maintain a reduction factor of 0.5, regardless of the S/D ratio. In contrast, BD-620M adopts for all bridges, regardless their S/D ratios, the most conservative drag coefficient distribution model provided by (AASHTO 2017), originally intended for S/D greater than 3. It should be noted that the wind pressure distribution follows the drag coefficient distribution model, so the terms can be used interchangeably.

A comparison between the PennDOT and AASHTO wind loading procedures can now be performed considering their entire process. First, for S/D less than or equal to 3, the discrepancies between AASHTO and PennDOT processes mainly depend on the number of girders in the girder system, owing to the variation in base wind pressure and wind pressure distribution model utilized. These discrepancies have been identified by examining the maximum lateral displacement of representative bridges when subjected to AASHTO and PennDOT drag wind pressure, as described in Chapter 4. In general, the PennDOT procedure is found to be more conservative, that is, it results in larger lateral displacements than AASHTO for girder systems with 4, 5 and 6 main girders, which are the most typical cases. However, the opposite is found for the less common configurations with 2, 3, 7 and more girders, that is AASHTO is more conservative than PennDOT in these cases. Considering the specific scenario for bridges over traffic and under construction, the PennDOT's procedure is found to be more conservative than that provided by AASHTO for the cases with S/D less than or equal to 3, except for the less common configuration of 2 girders. Additionally, for the less common case of S/D greater than 3, the lateral displacement from the PennDOT wind loading procedure is again found to be less conservative than the AASHTO procedure. This is because PennDOT employs lower base wind pressure values than AASHTO, while in this case both standards use the same wind pressure distribution model, with a wind pressure reduction factor of 0.5 for the third and subsequent girders. These assessment findings are also supported by the results of the parametric study performed in Chapter 4, as subsequently discussed.

The PennDOT lateral stability bracing guidelines outlined in the BD-620M standard (PennDOT 2019a) have also been examined in this report and findings are now summarized here. These guidelines are based on a defined permissible lateral displacement of $L/150$, where L is the girder span, and their detailed description can be found in Chapter 2. To assess these guidelines a parametric study has been performed considering all relevant parameters involved in wind loading, structural modeling, and analysis. Chapter 3 offers the details of the structural modeling, by showing the considered structural elements, supports, and connections, in addition to the structural analysis procedures. A case study bridge girder system has been analyzed, to provide a specific example of the involved wind loading and structural modeling and analysis. This analysis has also been utilized to verify the considered structural modeling and analysis procedures. A key point is that BD-620M recommends modeling the transverse diaphragm connections as pinned connections in the plane of the girder system. The impact of fixed and partially fixed transverse diaphragm connections on lateral displacement has been investigated in Chapter 3. The results of this investigation indicate that the lateral displacement of the girder systems is highly sensitive to the degree of connection fixity. However, the pin connections, as currently recommended, are conservative and anything other is either difficult to quantify for modeling (partial fixity) or likely not practical (fully fixed).

Having verified the structural modeling and analysis approaches, a parametric study has been performed in Chapter 5. Numerous girder systems with different parameter values have been analyzed, with a particular emphasis on comparing the lateral displacement of the girder systems against the permissible values of $L/150$. The parametric study results revealed that braced girder systems exhibit lateral displacements that are well below the permissible $L/150$ limit, emphasizing the effectiveness of lateral bracing in suppressing such displacements. In contrast, the unbraced girder systems modeled with pinned transverse diaphragm connections have lateral displacements that in most cases exceed the allowable limit, except for the studied single-span bridges with span lengths less than 150 ft. Despite the fact that the fixed connections result in lateral displacements that fall below the allowable limit, it is noted that achieving fixed connections might not be practical in most situations, often due to the bridge design or construction procedures. Furthermore, a pinned connection is both conservative, in terms of resulting in the largest displacement values relative to any increase in the degree of rotational fixity, and a more reliable modeling assumption relative to partial fixity (difficult to quantify) or fully fixed connections (likely not practical).

An investigation of the impact of the wind uplift forces on the girder system demands has also been performed in Chapter 3. The results of this investigation indicated that the lateral displacement of the girder system is not affected by wind uplift forces, and that the total wind uplift force is insignificant when compared to the self-weight of the girder system. Moreover, the study found that the girder system is not susceptible to overturning instability as a result of vertical uplift wind forces.

Based on the findings of this study, a potential adoption of the AASHTO procedures in BD-620M, either fully or only for computing the base design wind pressure values, could be investigated further in a possible future work.

5.2 Recommendations

Based on the aforementioned efforts, summary and conclusions, it is determined that the current PennDOT's wind loading procedure for wind loading on completely erected steel girders with diaphragms installed, yet prior to the placement of the deck, is slightly more conservative than AASHTO's Guide Specifications for Wind Loads During Construction (AASHTO 2017) for the typical cases of bridges with 4, 5 and 6 main girders and girder spacing to girder depth (S/D) less than or equal to 3.

However, estimation of wind loads following the AASHTO Guide Specifications for Wind Loads During Construction 2017 (AASHTO 2017) results in more conservative lateral displacements in comparison to BD-620M for the following less common configurations:

    i) Cases of S/D greater than 3.

    ii) Cases with 2-3 girders and S/D less than or equal to 3.

    iii) Cases with 7 or more main girders and S/D less than or equal to 3.

For bridges over traffic and under construction, the PennDOT BD-620M standard considers 5 psf of additional wind pressure, resulting in AASHTO specifications being more conservative only in the following cases:

    i) Cases of S/D greater than 3.

    ii) Cases with 2 girders and S/D less than or equal to 3.

In all other cases for bridges over traffic and under construction, PennDOT's specifications are more conservative.

Based on the results of this study, it is also determined that it is not necessary to consider uplift wind loading simultaneously with lateral wind loading for straight girder systems with a 90-degree skew angle, when estimating lateral displacements of girder systems during construction.

Suggested revisions of PennDOT's BD-620M could include the following:

    a) Revision of the statement "Evaluate the need for lateral bracing for spans in excess of 200 ft. based on lateral deflection." as follows: "Evaluate the need for lateral bracing for spans in excess of 150 ft. based on lateral deflection."

    b) Revision of the statement "Girders shall be designed so that no lateral bracing is necessary for girder spans less than 200 feet, ratio of girder spacing over girder depth less than or equal to 2 and a bridge cross section with 4 or more girders. The engineer will evaluate the dead load plus wind condition with an unbraced top flange, and if necessary, modify the girder design." as follows "Girders shall be designed so that no lateral bracing is necessary

for girder spans less than 150 feet, ratio of girder spacing over girder depth less than or equal to 2 and a bridge cross section with 4 or more girders. The engineer will evaluate the dead load plus wind condition with an unbraced top flange, and if necessary, modify the girder design."

c) Revision of the statement "Wind load per foot of bridge is (girder depth + deck thickness at fascia girder) x design wind pressure. Only the fascia girder will be loaded." as follows "Wind load per foot for each main girder is the girder depth x design wind pressure computed for this girder.

References

AASHTO. 2015. *AASHTO LRFD Bridge Design Specifications*. American Association of State Highway and Transportation Officials.

AASHTO. 2017. *AASHTO Guide Specifications for Wind Loads on Bridges During Construction*. American Association of State Highway and Transportation Officials.

AASHTO. 2020. *AASHTO LRFD Bridge Design Specifications*. American Association of State Highway and Transportation Officials.

ADINA. 2012. *Theory and Modeling Guide, Volume 1: ADINA Solids & Structures.*

ASCE/SEI. 2010. *Minimum Design Loads for Buildings and Other Structures, ASCE/SEI 7-10.* American Society of Civil Engineers.

ASCE/SEI. 2022. *Minimum Design Loads and Associated Criteria for Buildings and Other Structures, ASCE/SEI 7-22*. American Society of Civil Engineers.

Consolazio, G. R., and Edwards, S. T. 2014. *Determination of Brace Forces Caused by Construction Loads and Wind Loads During Bridge Construction*. Department of Civil and Coastal Engineering, University of Florida.

Consolazio, G. R., Gurley, K. R., and Harper, Z. S.. 2013. *Bridge Girder Drag Coefficients and Wind-related Bracing Recommendations*. Department of Civil and Coastal Engineering, University of Florida.

CSI. 2021. *SAP2000 Integrated Software for Structural Analysis and Design*. Computers and Structures Inc.

Hibbeler, R. C. 2017. *Structural Analysis*. Pearson.

NHI. 2015. *Engineering for Structural Stability in Bridge Construction, FHWA-NHI-15-044*. Reference Manual for NHI Course Number 130102, National Highway Institute, Federal Highway Administration.

PennDOT. 2010. *Bridge Construction, BC-772M Standard*. Pennsylvania Department of Transportation.

PennDOT. 2010. *Bridge Design, BD-620M Standard*. Pennsylvania Department of Transportation.

PennDOT. 2016. *Bridge Design, BD-620M Standard*. Pennsylvania Department of Transportation.

PennDOT. 2019a. *Bridge Design, BD-620M Standard*. Pennsylvania Department of Transportation.

PennDOT. 2019b. *Design Manual, Part 4 (DM-4)*. Pennsylvania Department of Transportation.

PennDOT. 2020. *Publication 408/2020, Specifications*. Pennsylvania Department of Transportation.

Peterka, J. A., and Shahid, S. 1998. *Design Gust Wind Speeds in the United States*. J. Struct. Eng., 124 (2): 207–214.

Simiu, E., and Scanlan, R. H. 1997. *Wind Effects on Structures: Fundamentals and Applications to Design*. John Wiley New York.

Vickery, P. J., Wadhera, D., Galsworthy, J., Peterka, J. A., Irwin, P. A., and Griffis, L. A. 2010. *Ultimate Wind Load Design Gust Wind Speeds in the United States for Use in ASCE-7*. J. Struct. Eng., 136 (5): 613–625.

Wassef, W., and Raggett, J. 2014. *Updating the AASHTO LRFD Wind Load Provisions*. Final Report for NCHRP Project 20-7, Task 325, Transportation Research Board, National Research Council.